

# An Ultrasonic Atomisation Unit for Heat and Moisture Exchange Humidification Device for Intensive Care Medicine Applications

Mahmoud Shafik

**Abstract**— The state of the art of the existing heat and moisture exchange (HME) technology in use concludes that there are two main artificial humidification HME devices: active and passive device. The active device is complicated to use and expensive. The passive HME device is the preferred one, due to the ease of use and low cost. However it is not suitable for more than 24 hour use. This is due to current devices cavity design, limitations of HME materials performance and overall device efficiency. This paper presents the outcomes of the research work carried out to overcome these teething issues and presents a piezoelectric ultrasonic atomisation device for passive humidification device. This aims to improve the device heat and moisture exchange (HME) materials performance, by recovering the accumulated moisture, for a greater patient care. The atomisation device design, structure, working principles and analysis using finite element analysis (FEA) is discussed and presented in this paper. The computer simulation and modeling using FEA for the atomisation device has been used to examine the device structure. It also enabled to select the material of the active vibration transducer ring, investigate the material deformation, defining the operating parameters for the device and establish the working principles of atomization unit. A working prototype has been fabricated to test the device, technical parameters, performance and practicality to use in such intensive care applications. Experimental tests showed that the electrical working parameters of the device are: Current: 50 m-amps, Voltage: 50 volts, Frequency: 41.7 kHz. The atomization device has been integrated into the passive HME humidification device and initial results show some improvement in moisture return of the device by 2.5 mg per liter H<sub>2</sub>O. This shows the potential of the developed unit to improve the HME material performance in such working environment.

**Index Terms**— Humidification Device, Heat and Moisture Exchange Medication Devices, Piezoelectric Ultrasonic Atomisation Unit.

## I. INTRODUCTION

Smart materials and its utilization in actuation technology is evolving so fast. Careful consideration of its implantation could make a big difference in our daily life, especially in medical and intensive care applications. Humidification is an essential function of the nose and mouth for human beings, to ensure normal health and function of the respiratory system. During surgery and inside the intensive care unit after a major

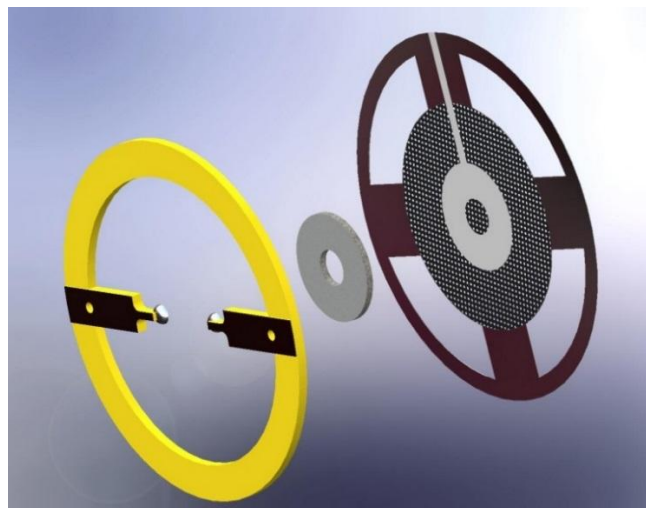
operation, the patient upper airway tract is bypassed to assist breathing and enable controlled delivery of medical gases and thus artificial means must be used for humidification [1-4]. The state of the art of existing technology in use concludes that there are two main artificial humidification heat and moisture exchange (HME) devices: active and passive device. The active device is complicated to use and expensive. The passive HME device is the preferred one, due to the ease of use and low cost. However it is not suitable for more than 24 hour use. This is due to a number of challenges such as: current devices design, limitations of HME materials performance and overall device efficiency [3-9].

Smart piezoelectric ultrasonic actuation principles of operations are based on the concept of driving the rotor by a mechanical vibration force generated on the stator via piezoelectric effect. The stator is mainly made of Lead Zirconate Titanate (PZT) Transducer. Ultrasonic actuators can be classified into two main categories, based on the PZT working mode. These are the bonded type actuators [3-9] and the bolt-clamped type actuators [10-12]. Ultrasonic actuators have compact size, high force density and simple mechanical structure, slow speed without additional gear or spindle, high torque, non-magnetic operation, freedom for constructional design, very low inertia, fast dynamic time responses, direct drive, fine position resolution, miniaturization and noiseless operation. These criteria gave them the potential to be used in a number of industrial applications [13-21].

Demanding and careful examination for such applications reveals that there are apparent teething issues with these actuators technology. The first issue is in regard to the dynamic response of the actuators and its transfer function. While a piezo-ceramic element, typically PZT, expands in direct proportion to the magnitude of the applied voltage, the ultrasonic actuators on the other hand accumulates those displacements over time. Therefore the transfer function of the actuators, relating to the magnitude of the driving signal to the displacement is an integrator [18, 21-22]. This is why there was a delay in the dynamic response of the ultrasonic actuators. The second issue is ultrasonic actuators motion is generated through a friction force between solid elements therefore it has a dead band. Often ultrasonic actuators do not move until the input signal is greater than 10% of the maximum input voltage to overcome the friction. This dead band limits the ability of ultrasonic actuators to accelerate quickly [3, 21-22].

## II. PIEZOELECTRIC ULTRASONIC ATOMISATION UNIT STRUCTURE

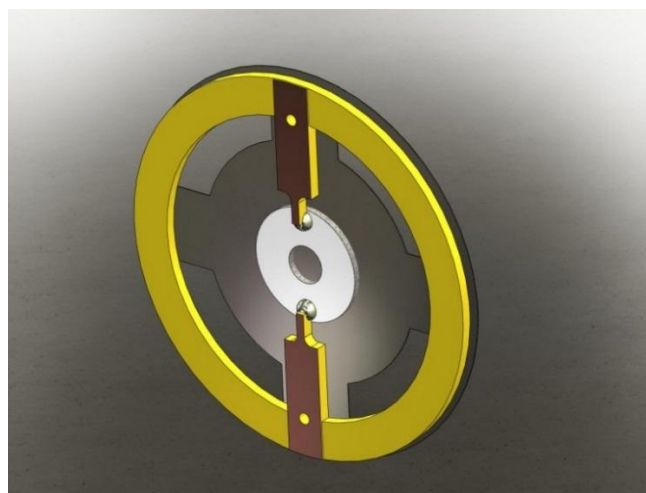
Fig 1. shows the structure of the piezoelectric ultrasonic atomisation unit. Fig 1 (a) and (b) show the unit main components and the assembled CAD design of the unit, respectively. The unit consists of three main components which are the active piezoelectric ultrasonic transducer element, disk and printed circuit board (PCB) ring. The active element is a single flexural vibrating ring made from piezo-ceramics PZT material. The disk is made from steel and has been micro machined with array of micro holes using advanced in Nano and micro laser machining technology. The PCB ring is made from fiber and this is to house the piezoelectric ultrasonic atomisation unit to the passive HME humidification device.



(a)

## III. PIEZOELECTRIC ULTRASONIC ATOMISATION UNIT WORKING PRINCIPLES

The concept of the working principles of the under development piezoelectric ultrasonic atomisation unit is based on longitudinal and transverse, which has a fixed wave length. The concept is to utilise the two oscillation modes to obtain desired forward and backwards motion of the piezoelectric actuation element. These motion will help to extract the absorbed moisture by the HME material. One vibration produces a normal force while the other vibration generates thrust force, which is perpendicular to the normal force, resulting in a micro elliptical trajectory of the element edge, by attaching the piezoelectric ceramic ring to a micro machined steel dish as shown in Figure 1-(b). The micro elliptical trajectory driving force is converted into a movement in forward and backward directions, with force strength depending on the methodology used to electrify the piezoelectric ceramic transducer ring to generate two modes of vibrations, at the resonance frequency.



(b)

Figure 1: Design and structure of the ultrasonic atomisation unit (a) unit components (b) overall assembled structure of the unit

## IV. MODELLING AND ANALYSIS OF THE PIEZOELECTRIC ULTRASONIC ATOMISATION UNIT

Modelling and analysis of ultrasonic actuators and atomisation devices have many complex non-linear characteristics. Commonly two methods of analysis can be used to simulate and modal such types of devices [13-18, 21-23]. These methods are the analytical analysis and finite element analysis (FEA) method. Here FEA has been used in the actuator design process, to test the unit design structure, investigate the material deformation i.e. vibration modals (longitudinal and bending modes). Samples of the data used in the proposed actuator modelling are illustrated in tables 1 and 2. The piezoelectric ultrasonic vibration ring transducer is arranged as shown in Figure 2-(a). Figure 2-(b) shows the variation of the displacement of the PZT Transducer ring versus exciting frequency, of the active transducer. This shows the natural frequency of the proposed atomisation unit design structure and is equal to 42.2 KHz. It also shows the possible maximum displacement amplitude and this is equal 0.70 micrometer at 50 volts.

The natural frequency indicates the dynamic response of the piezoelectric ultrasonic actuation element and in this case it is found in the order of microseconds. This can be calculated roughly as Q times the vibration period. Where Q is the quality factor of the motor and it can be determined using the following relationship [14-18, 24-25]

$$Q = \frac{R_m}{\sqrt{\frac{L}{C_\Sigma}}} \quad (1)$$

Where,  $R_m$  is the equivalent resistor of the vibration transducer at a fixed operating frequency. L is the inductance

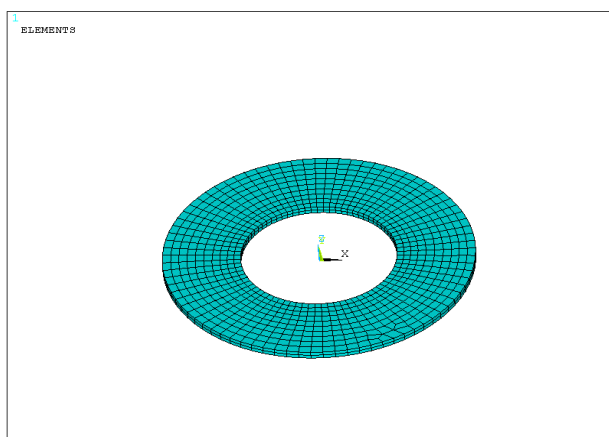
of the LC-driving circuit.  $C_\Sigma$  is the total capacitance which is not constant and is depend on the vibration transducer internal capacitance, cable internal capacitance and LC-driving circuit capacitance.

Table 1 LZT-PC4D Piezo-ceramic material used for piezoelectric ultrasonic Atomisation unit

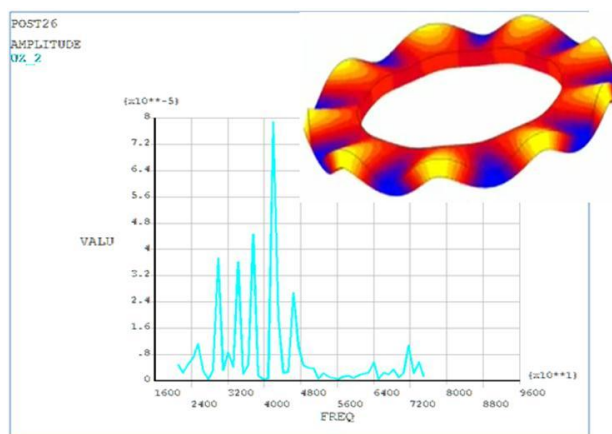
Material	Coefficient	Value
LZT-PC4D	Relative permittivity ( $\Omega m$ )	1325
	Dielectric loss ( $\Omega m$ )	0.002
	Resistively ( $\Omega m$ ) $\times 10^{12}$	10
	Quality factor	1600
	Density ( $kg/m^{-3}$ )	7550
	Poisson's ratio	0.33
	Coupling factor	0.7

Table 2 Transformation of E-coefficient to D-coefficient for Piezo-ceramic material used for Piezoelectric Ultrasonic atomisation unit

Material	Coefficient	Value (m/v)
Piezo-ceramics	$d_{13} \times 10^{-12}$	100
	$d_{33} \times 10^{-12}$	200



(a)



(b)

Figure 2: (a) Atomisation unit piezoelectric ultrasonic (PZT) transducer FEA Model (b) variation of the transducer displacement vs. the exciting frequency

## V. MODELLING AND ANALYSIS OF THE HME DEVICE AND ATOMISATION UNIT

Figure 3 shows the structure of the passive HMS humidification device. The device is composed of a plastic

moulded cavity, in two halves enclosing successive layers of materials. These materials include: A filter restricting the passage of contaminants, bacteria and viruses, Heat and moisture exchange materials operating through the sorption of heat and moisture during exhalation, and the desorption of heat and moisture during inhalation, the piezoelectric atomisation incorporating piezoceramic element, a thin metal plate and a wick feed system enabling vibration of the metal plate at ultrasonic frequencies, thereby resulting in re-aerolisation of captured moisture.

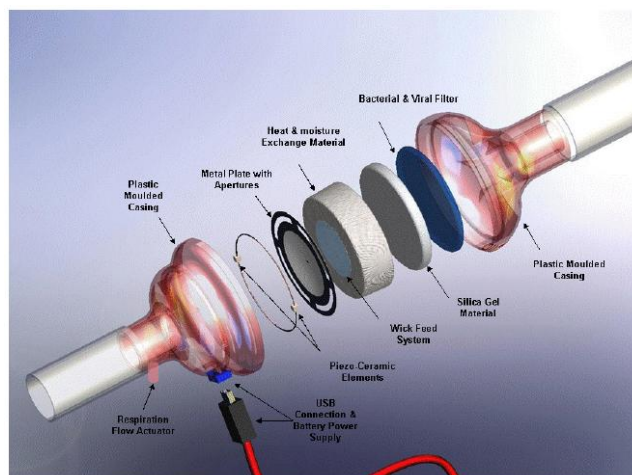


Figure 3: HME humidification device, main units, mechanical and electrical interfaces [1-2]

### A. Plastic Casing Oval Shape, Filter, HME Material & Ultrasonic Atomisation Unit

Figure 4 shows the HME humidification device assembly include the ultrasonic atomisation unit placed on the top of the HME material. I.e. the unit will be integrated into the device cavity and placed in the patient side. This unit function is to recover the moistures captured in the HME material.

The airflow direction is mainly dictated by the geometry of the piezoelectric atomisation unit. This unit integrates a 30mm diameter nebulising mesh with  $<6\mu m$  sized holes (porosity of 20%) sitting in the middle of the 58mm wide. A piezo-ceramic ring with a 5mm bore is centred on the mesh surface. The air will flow without restriction through the holes outside the mesh and with a resistance to flow (proportional to the porosity) through the mesh outside the piezo-ceramic element which does not allow air to flow through its surface.

Figure 5 shows the Analysis of the fully assembled device and pressure build up early in the device. It show how the atomisation unit has affected the pressure distribution, air flow and air pattern structure within the device cavity.

Figure 6 (a) and (b) shows the air flow analysis within the device and the limitations brought in by the piezo nebuliser. The inner ring hole overshadowing a mesh area does not allow sufficient air to flow directly through the central part of the device. The remaining air fed to the device is deviated to the area around the piezo ultrasonic ring. As can be seen in Figures 6 to 8, the air flows smoothly through both the meshed area and the outside hollow areas, before penetrating into the HME materials then the filter along the parallel direction to the central axis. Figure 9 shows the turbulence



analysis and the turbulences created around the piezo element. The pressure flow through the HME material and the filter is relatively homogenous as dictated by the piezo-nebuliser (Figure 10). It appears that there is only little problem for the air to exit the device smoothly.

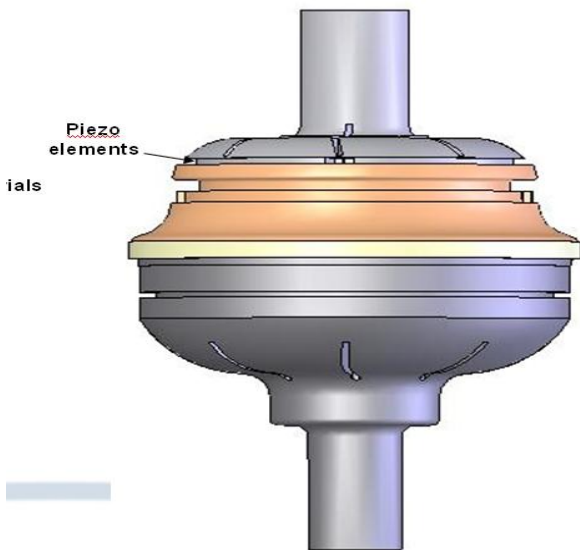


Figure 4: Passive HME humidification device fluid domain in cavity, Filter, HME material and atomisation unit

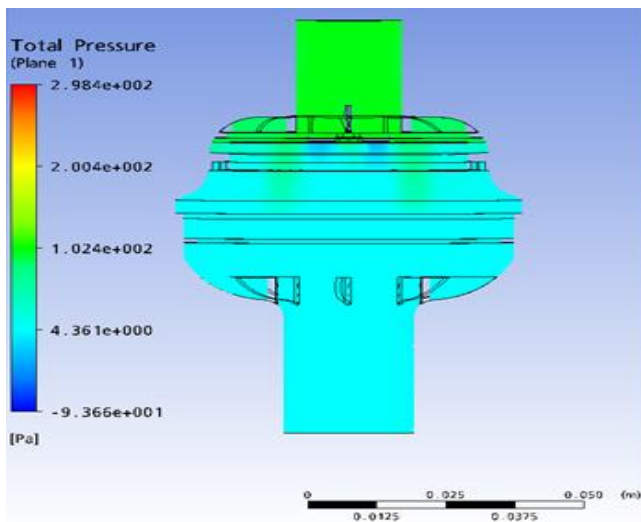
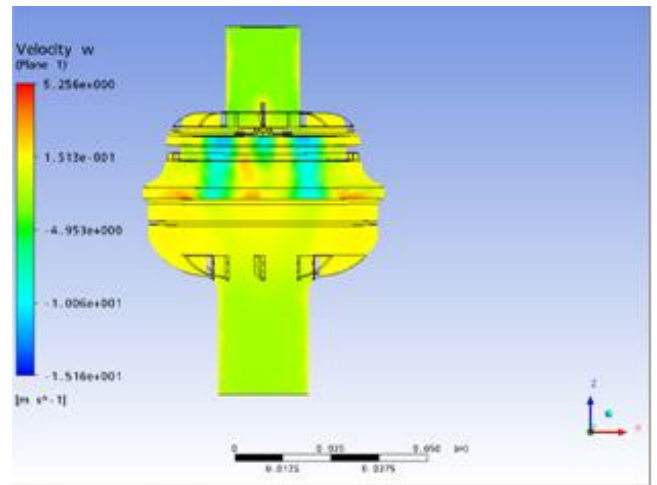


Figure 5: Finite Element Analysis and pressure distribution for the internal volume of the plastic moulded casing and other components integrated into the HME device

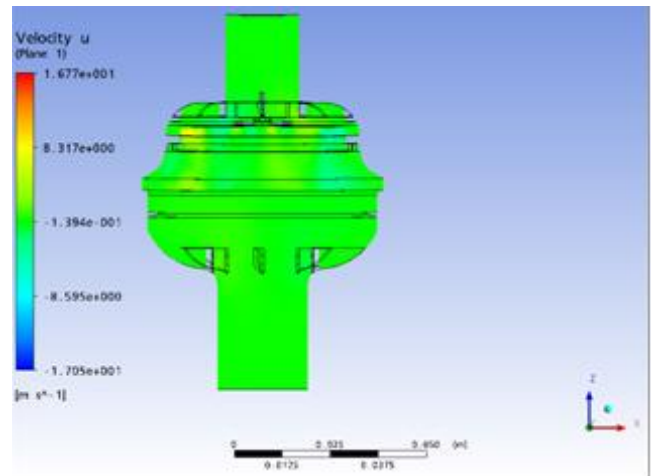
**B. Plastic Casing tube shape, Filter, HME Material & Piezo-Nebuliser**

Due to the more restricted diameter of the device, the piezo-aerosoliser studied only included a mesh (with  $<6\mu\text{m}$  sized holes) and a piezo-ceramic element centred on its surface. As for the first optimized output the presence of the piezo element ring considerably restrict the airflow through the centre of the device. It is also noticed that the remaining cavity space allow for the rest of the flow is also reduced. This is leaded to an immediate increase in the pressure before the piezo-nebuliser. This is clearly shown in Figure 11. Once the air passed this restricting area, it follows the shortest way

to the tube exit. It flows in parallel to the tube axis through the HME materials and the device filter (Figures 12 to 14). The fluid is therefore mainly concentrated in both sides of the cavity and in the centre of the device.



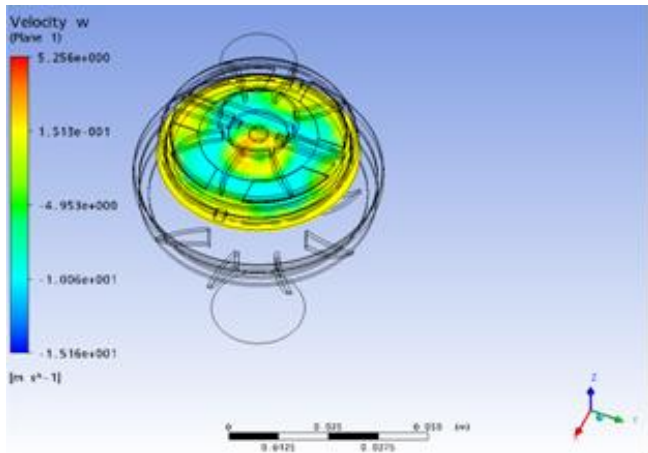
(a)



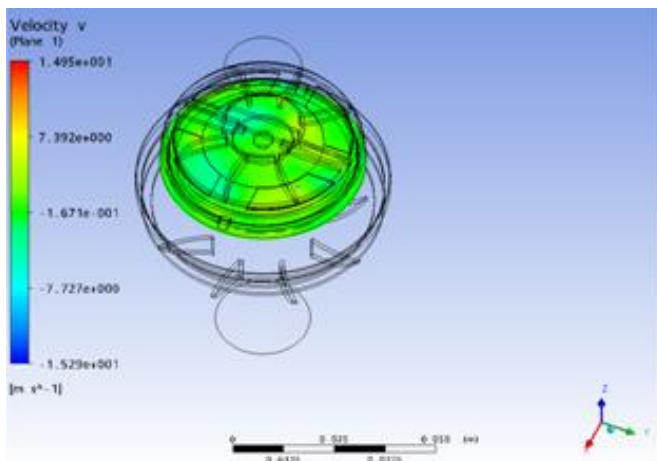
(b)

Figure 6: HME device velocity distribution incorporating a Filter, HME Material and ultrasonic atomisation unit a) Vertical airflow and b) Horizontal airflow

Similarly to the first proposed model, important turbulences are created as the air has to flow around the piezo element; however, due to the higher pressure on the patient's side of the filter, a higher level of turbulences is generated. In fact the addition of the piezo-nebuliser created a large flow restriction in the device increasing the pressure drop in the device from an average of 92.5 Pa in the ID 22mm connector device to 136 Pa in the latest device. Despite increased pressure, the air flowing through the tubular device will flow through a much larger volume of HME material and might therefore keep a significant advantage in term of heat and moisture exchange. Since the piezoelectric atomisation used in the CFD analysis had been designed based on the initial design, it is possible that a better piezo-element could be incorporated to the tubular design that would not affect the air flow to that extend (maybe using a more porous mesh or reducing the area covered by the piezo ceramic).



(a)



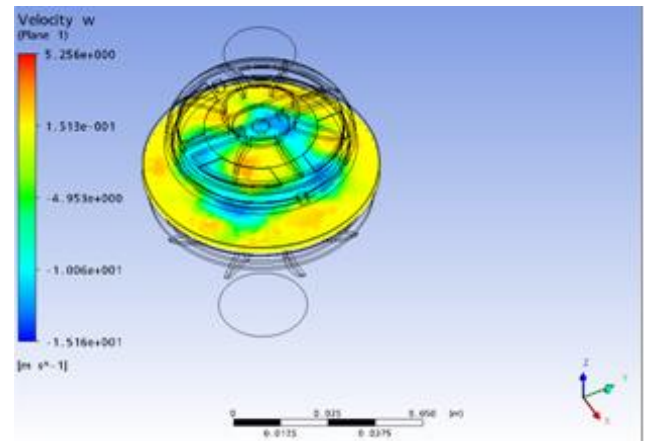
(b)

Figure 7: HME device distribution of the airflow velocity at half height of the HME Material (a) Vertical airflow (b) Horizontal airflow

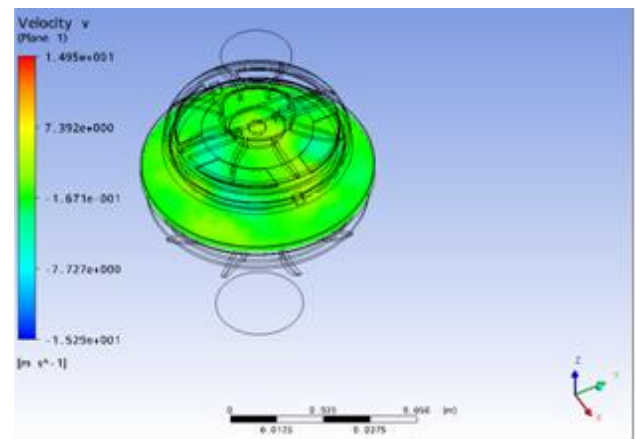
Simulations carried out on the initial design showed airflow mainly concentrated in the centre of the device, leading to a limited utilisation of the HME materials in the sides of the cavity. Integration of the filter and HME material in the device demonstrated a slightly improved airflow spread. However, these additional components did not homogenise the airflow to the HME material in the device. Another significant problem also observed in the initial design was the pressure build-up and resistance to flow observed in the bottom of the device. This was due to the significant decrease of the outlet diameter. The widening and tapering of the inlet and outlet improve the airflow distribution through the cavity leading to a higher utilisation percentage of the HME material. This should lead to improved heat and moisture exchange properties. Analysis of a potential device with these modifications showed a potential reduction by a factor of 7 of the pressure drop between the inlet and the outlet [1-2].

Alternative humidification devices have been designed and are being analysed to further optimise the airflow distribution within the cavity and generate improved airflow patterns over target HME material structure. Enlarging the device input and output connector to allow easier access to air in and out of the device. This is largely increased the theoretic potential of the initial device. However, this did not suffice in optimising the

air flow through the HME materials. Furthermore, the holes on the outside of the mesh might lead to the HME material releasing water but not as an aerosol while by-passing the nebulising mesh.



(a)



(b)

Figure 8: HME device distribution of the airflow velocity in the middle of the Filter (a) Vertical airflow (b) Horizontal airflow

A different design was considered to facilitate the flow through the HME materials in a homogenous manner, to improved heat and moisture exchanged properties and reduce the resistance to flow within the device. However, the addition of the piezo-nebuliser still created a large flow restriction in the device and increased the pressure drop in the device from an average of 92.5 Pa in the ID 22mm connector device to 136 Pa in the latest device.

Despite increased pressure, the air flowing through the tubular device will flow through a much larger volume of HME material and therefore keep a significant advantage in term of heat and moisture exchange. Since the nebuliser used in the CFD analysis had been designed based on the initial design. It is possible that a better piezo-element could be incorporated to the tubular design that would not affect the air flow (i.e. using a more porous mesh or reducing the area covered by the piezo ceramic). The results for the analysis presented in this paper are summarised in table 3 below.

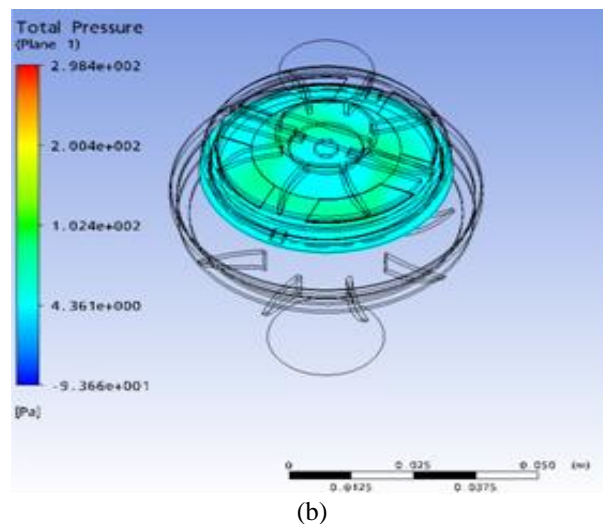
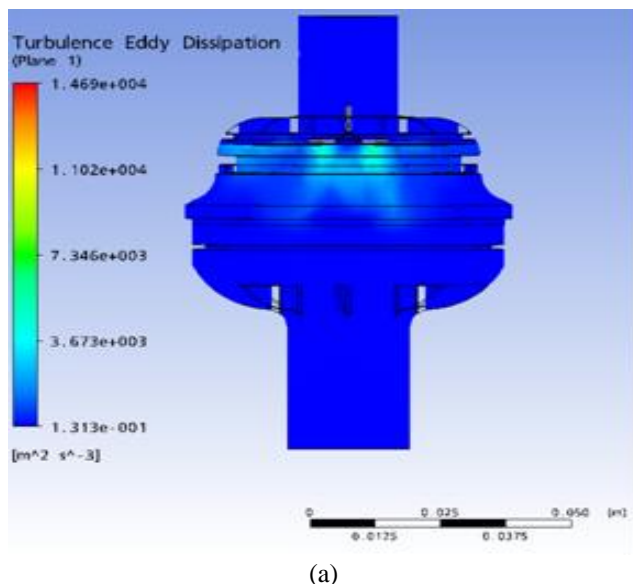


Figure 10: HME device pressure distribution a) in the middle of filter b) at half height of the HME material

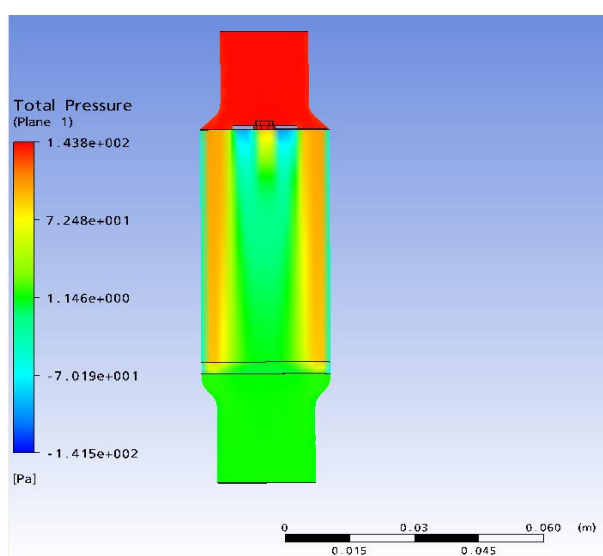
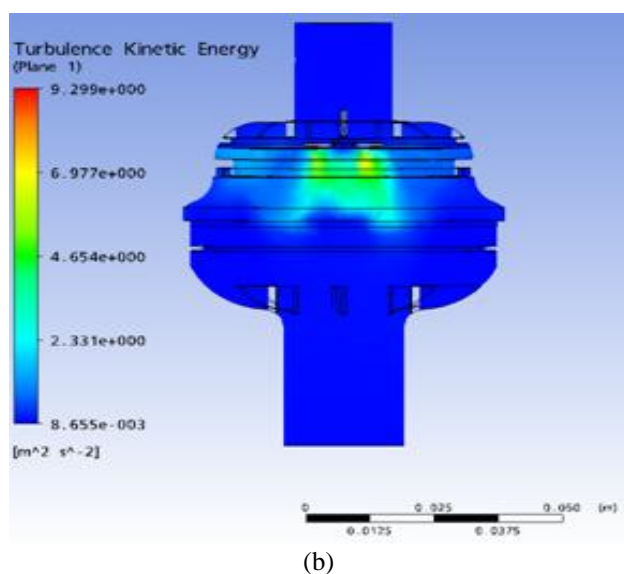
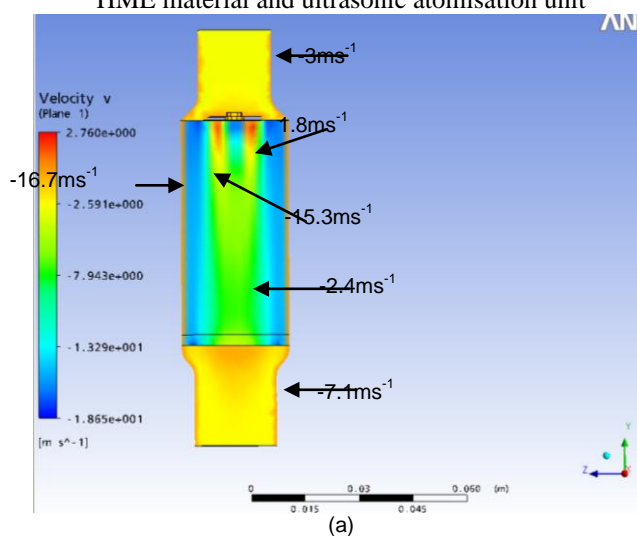
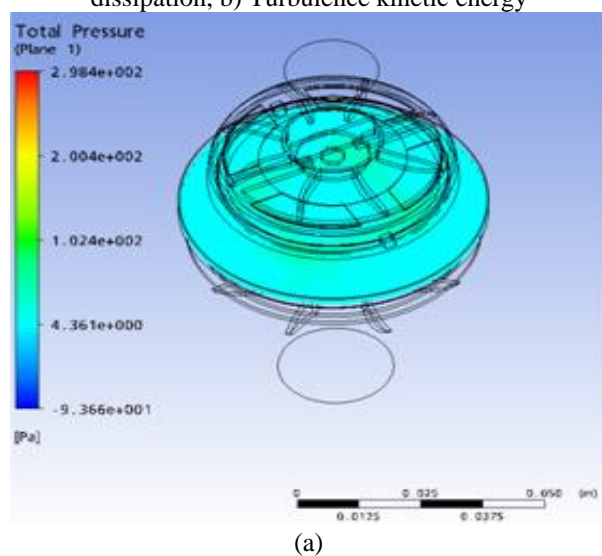
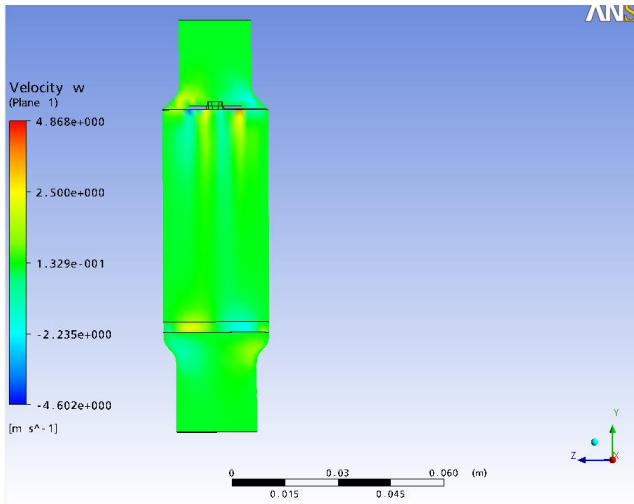


Figure 11: HME device pressure distribution for the internal volume of the plastic moulded casing incorporating a filter, HME material and ultrasonic atomisation unit

Figure 9: HME device Turbulence-a). Turbulence eddy dissipation, b) Turbulence kinetic energy

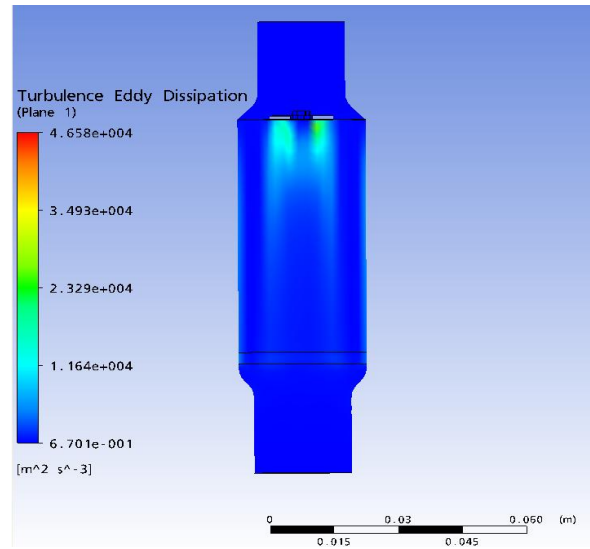




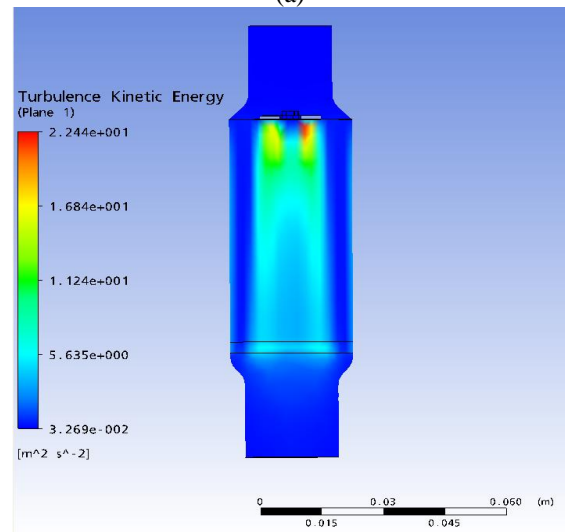


(b)

Figure 12: HME device Velocity distribution for the internal volume of the plastic moulded casing incorporating a filter, HME material and ultrasonic atomisation unit

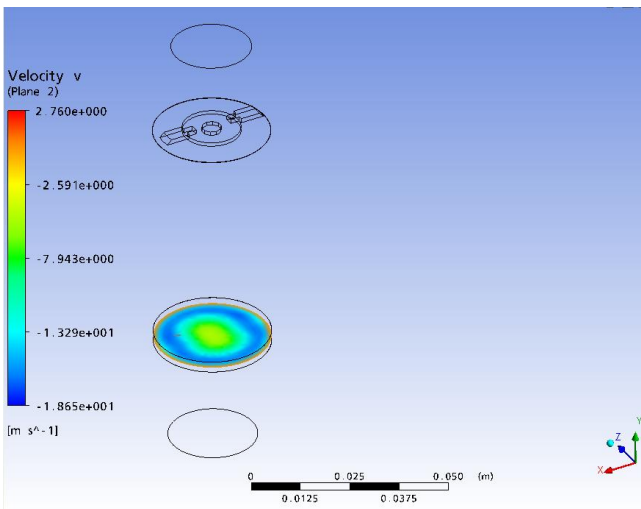


(a)

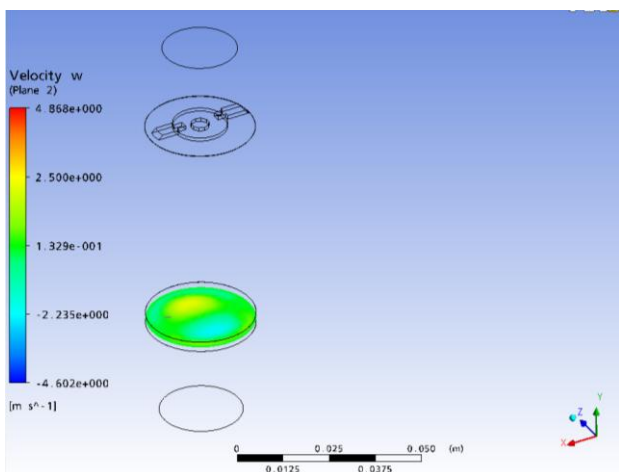


(b)

Figure 14: HME device Turbulence-a). Turbulence eddy dissipation & b) Turbulence kinetic energy



(a)



(b)

Figure 13: HME device Distribution of the airflow velocity in the middle of the filter a) Vertical airflow b) Horizontal airflow

Pressure and temperature are two important parameters that will affect the ability of the HME material to absorb and desorb moisture (expired air will be hot and pressurized while inhaled air will be at room temperature and under minimal pressure - unless under artificial ventilation as the pressurizations would be inverted). The behaviour of the material in correlation with these parameters is not theoretically known and will need to be tested experimentally. The identification of an HME material that will take advantage of these different conditions will be beneficial to the device. Depending on properties of the HME material used in the device, one design might be more efficient than the other.

Table 3: Results for the pressure drop for different designs and materials arrangement

Initial Design	Pressure drop (Pa)
Casing	35.6
Casing & filter	113.8

Casing, filter & HME	197.3
Ø22mm inlet & outlet optimized design	
Casing	0.21
Casing & filter	52.9
Casing, filter & HME	67
Casing, filter, HME and piezo-nebuliser	92.3
<b>Second alternative design: Long tube</b>	<b>Pressure drop (Pa)</b>
Casing	0.72
Casing & filter	46.24
Casing, filter & HME	79.76
Casing, filter, HME and piezo-nebuliser	136.1

#### VI. EXPERIMENTAL TESTS, RESULTS AND DISCUSSIONS

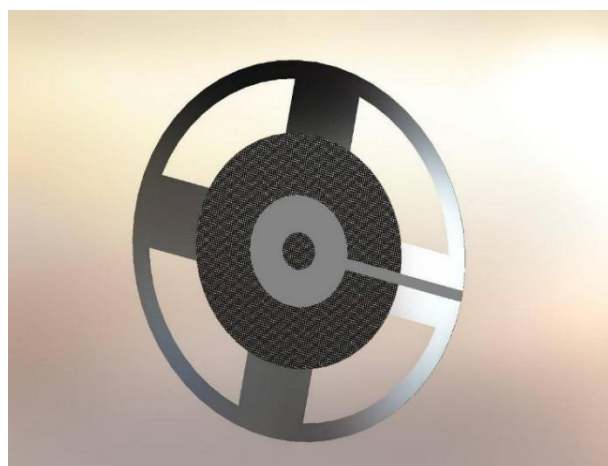
In the first stage of the experimental test the atomisation unit has been fabricated and assembled. Figures 15 (a) and (b) show the piezoelectric ring integrated to the PCB ring and Figure 15 (c) shows the actual piezoelectric ultrasonic atomisation unit prototype. The necessary units for testing atomisation device have been identified. The units include piezoelectric amplifier driver, aperture plate with different sizes and few samples of filtration media filter saturated with some moisture. Figure 16 shows actual ultrasonic atomisation unit prototype under testing using off shelf piezoelectric ultrasonic drive. The initial test to the developed unit shows that the operating frequency, internal parasitic capacitance, driving power and force are the most important parameters to be carefully considered. This also showed that the electrical working parameters of the device are: Current: 50 m-amps, Voltage: 50 volts, and Frequency: 41.7 kHz.

The advance in airflow, humidification sensing and electronics was fully investigated and some of the necessary sensors and instrumentation have been identified. This considered many technical parameters such as application resolution, sensitivity and dynamic time response. An investigation to the artificial breathing mechanism was also necessary to define most of the system relevant parameters. This shows that typical patient ventilation pressures are 0 - 40cm H<sub>2</sub>O, Maximum pressure under ventilator testing and circuit testing is 120cm H<sub>2</sub>O.

Typical flow rates ventilating a patient are 5 - 30lpm, Maximum flow in a disconnect situation approx. 18lpm and typical adult breathing pattern would be 10-20 breaths per minute, 300-600 ml tidal volume (the volume of each breath) Inspire to Expire ratio of 1:2 (breath in is 2x faster than breath out).



(a)



(b)



(c)

Figure 15: Fabricated ultrasonic atomisation unit elements (a) ring attached to the PCB ring (b) the disk with array of micro machined holes (c) assembled prototype

##### A. Resistance to Flow Condition:

Condition the filter for duration of test using the gravimetric HME test rigs. As detailed in IWI1016, then record the pressure drop. Record the pressure drop at 60 l/min before and after test, according to IWI9300.

##### B. Resistance to Flow of Metal Discs:

The resistance to flow of a 1641 HME was measured and recorded at 60l/min as outlined in IWI9300. The HME device



was then opened and the metal disc inserted between the Foam HME and filter pad. The housing was then re-closed and the resistance to flow re-measured. Figure 17 shows the unit integrated into the passive humidification device cavity. Numbers of HME devices (Housing 1641 and 1341) with different material arrangement have been prepared (table 5) and then each one has been integrated into the Gravimetric HME test rig for testing. Figure 18 shows the test rig with various mentoring sensor, instrumentation and user friendly interface system with data logger. The user friendly interface screen developed; make it easy to interpret the system performance and humidification rate state. The initial tests show that the increase in resistance to flow was attributed to the disc. The resistance to flow of the full metal disc when sealed to the housing was also tested to get an actual reading of the resistance caused by the disc. This was achieved by gluing the disc around the un-perforated edge to the patient side of 1641 housing.

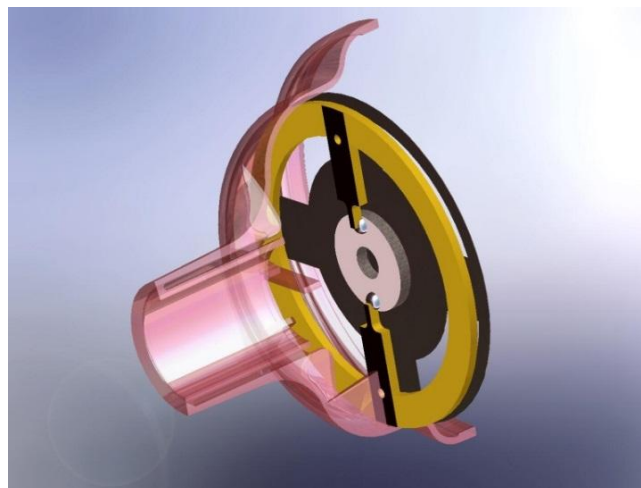


Figure 17: Atomisation unit integrated into the passive HME humidification device cavity

**C. Determination of Moisture Output:**

This should be performed as detailed in IW11016, recording an HME moisture output for the HME filter, at 500ml tidal volume. Resistance to Flow with full disc totally sealed = 2.4mb at 60l/min. Estimated time to reach saturation results: Weight gained by Hypol 1641 after 24 hours = 2.3g, Output of rig = 38mg/l, Efficiency of filter = 60% = 23mg/l. If the rig works at 10l/min then the estimated time to reach saturation ~ 10 minutes.

**D. Sources of Error:**

Determination of Moisture Output: Scales  $\pm 2\%$ , Gravimetric rigs  $\pm 1$  mg/l, Manometer  $\pm 0.05$ mbar and resistance to flow: TSI  $\pm 2\%$ .

**E. Resistance to flow of the metal discs:**

The added resistance to flow of the discs in the 1641 is well below the desired max fresh resistance of 3.0mb (table 4). However, when the full disc was sealed into the housing, then the resistance to flow is significantly higher, (2.4mb) and would cause an issue.

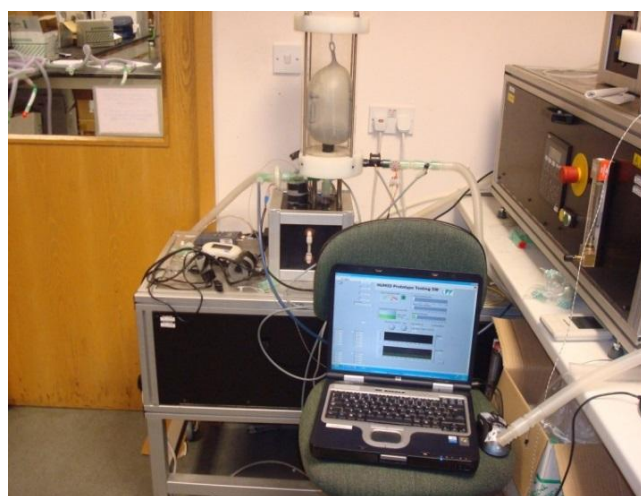


Figure 18: The test rig named Gravimetric HME with various mentoring sensors, instrumentation and user friendly interface system used to test ultrasonic atomisation unit integrated into HME device

**F. 1641 testing:**

Testing has shown that the Oasis media is probably unsuitable for use in a HME. When unsupported the media structure collapses in the presence of water causing initially the media to shrink and then that the material dissolves completely in water creating a gel. This is reflected in the very low moisture returns for the Oasis media (table 5).

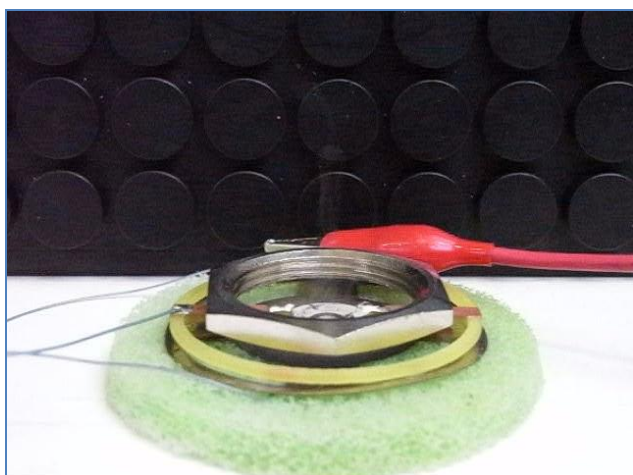


Figure 16: Developed ultrasonic atomisation unit prototype under testing using off-shelf piezoelectric drive and HME materials

Table 4: Perforated metal disc added resistance to flow at 60l/min

Disc	Resistance to flow (mb)
Full disc	0.9
Small windows	0.6
Large windows	0.3

Table 5: HME devices OFF moisture returns and fresh and conditioned resistance to flow

Test		Resistance to Flow (± 0.05mb)		Test Duratio n (± 0.05hrs)	Moisture Return OFF (±1 mg/l)
		Fresh	Conditio ned		
<b>1641 Housing</b>					
1	1641 Hypol Foam HME Pad	0.3	0.4	2.7	<b>22.8</b>
2	Oasis media	0.3	0.3	2.7	<b>12.2</b>
3	2 x Oasis Media	0.6	0.3	2.7	<b>10.8</b>
4	2 x H&V Filter Media	1.3	1.3	2.7	<b>15.8</b>
5	Oasis Media + Support Material	1.1	1.3	2.7	<b>21.1</b>
6	Silica Balls + 2 x H&V Filter Media	2.0	2.0	2.7	<b>18.2</b>
7	Piezo Off	4	4.2	22.7	<b>22.1</b>
7a	Piezo On	?	6.2	17.3	<b>24.6</b>
<b>1341 Housing</b>					
8	F-S-H	7.3	7.3	22.6	<b>30.8</b>
<b>9-1</b>	<b>P-F-S-H</b>	<b>5.1</b>	<b>5.4</b>	<b>16.7</b>	<b>27.0</b>
9-2	P-F-S-H	6.2	6.5	21.6	<b>33.3</b>
9a	P-F-S	4.9	5.7	21.7	<b>34.0</b>
10-1	P-S-F-H	?	7.5	18.2	<b>34.4</b>
10-2	P-S-F-H	5.6	6.0	21.5	<b>33.5</b>
10a	P-S-F	3.9	4.8	21.7	<b>33.7</b>
11	P-F (1341)	2.9	3.8	24.0	<b>32.0</b>

The test with the supporting media did however show that the Oasis will hold its shape if supported, in this instance by the threads between the media (5, table 5) the moisture return for this sample was significantly higher than without, (5, table 5) however without further testing it is unclear what, if any, contribution the oasis had and what is simply the return from the support media. The 1641 testing suggests that there is a benefit to using silica in the makeup of the HME element. Testing comparing with and without silica beads (5 and 6, table 5) showed an improved return with the beaded sample (6, table 4, ~2.5 mg/l improvement with beads). The beads kept their integrity after water contact. The significance of this one test is however low and many more tests should be run to verify the validity of these results.

Testing with the Piezo ultrasonic atomization unit enhanced 1641 showed that the piezo appeared to improve the moisture return of the device by 2.5 mg/l (7, table 5).

1341 Testing: The testing suggests that the combination of paper and silica (table 5) increases the performance of the existing paper/filter only HME (11, table 5), by approx. 1.5 –2mg/l. Testing appears to show that the addition of a heater has little effect on the moisture return, and could actually decrease the efficiency (9 and 10, table 5). 9-1 (highlighted red and bold) appears, because of its significantly lower performance, to be an anomaly in the testing and should therefore be discounted. The position of the filter pad in the arrangement does not appear to have a significant impact on

the HMEs performance (table 5). The estimated time for the 1641 HME to become saturated on the rigs is 10 minutes.

## VII. CONCLUSION

An ultrasonic atomisation device for passive HME humidification device intensive care and medical applications has been developed. The atomisation device design, structure, working principles and analysis using finite element analysis is discussed and presented in this paper. The computer simulation and modeling using finite element analysis for the atomisation device has been used to examine the device structure by performing an algebraic solution of a set of equations, describing an ideal model structure, with a finite number of variables. This is enabled to select the material of the activetransducer ring, investigate the material deformation, defining the operating parameters for the device and establish the working principles of atomisation unit. This is also helped to investigation the HME device air flow and pattern structure and possible influence such device could add to the system.

A working prototype has been fabricated to test the devicetechnical parameters, performance and practicality to be used in such applications. Experimental tests showed that the electrical working parameters of the device are: Current: 50 m-amps, Voltage: 50 volts, Frequency: 41.7 kHz.

The device integrated into the passive HME humidification device and initial tests results showed that the piezoultrasonic atomization unit appeared to improve the moisture return of the device by 2.5 mg/l.

There are still ongoing effort to improve the HME materials performance and the overall device efficiency and working service hours.

## ACKNOWLEDGEMENT

The authors would like to thank EC and HUMID consortium, for their support and dedication to deliver such an outstanding work and improve people quality of life. Especial thanks also go to Intersurgical Ltd, UK product development teams for their support and professional guidance during the project development lifecycle.

## REFERENCES

- [1] J. M. Shafik&Anne Lechevretel, (2014), ‘Computer Simulation and Modelling of Passive Humidification Device Cavity for Intensive Care Patient Medical Applications’, ASME 2014 International Mechanical Engineering Congress and Exposition, 14-20 of November, Montreal, Canada, Paper Number: IMECE2014-36505, 2014.
- [2] M. Shafik&Anne Lechevretel, (2014), ‘An Innovative Piezoelectric Ultrasonic Atomisation Actuator for Passive Humidification Device Intensive Care Patient Medical Applications’, ASME 2014 International Mechanical Engineering Congress and Exposition, 14-20 of November, Montreal, Canada, Paper Number: IMECE2014-36506, 2014.
- [3] Y. Chikata, J. Oto, M. Onodera, M. Nishimura, ‘Humidification Performance of Humidifying Devices for Tracheostomized Patients With Spontaneous Breathing: A Bench Study’, OPEN FORUM of the 58th AARC Congress, held November 10–13, in New Orleans, Louisiana, 2012.
- [4] Y. Chikata, C. Sumida, J. Oto, H. Imanaka, and M. Nishimura, ‘Humidification Performance of Heat and Moisture Exchangers for Pediatric Use’, Hindawi Publishing Corporation, Critical Care Research and Practice, Volume 2012, Article ID 439267, 5 pages, 2012.

- [5] G. Eason, B. Noble, and I. N. Sneddon, "On certain integrals of Lipschitz-Hankel type involving products of Bessel functions," *Phil. Trans. Roy. Soc. London*, vol. A247, pp. 529–551, April 1955.
- [6] J. Clerk Maxwell, *A Treatise on Electricity and Magnetism*, 3rd ed., vol. 2. Oxford: Clarendon, pp.68–73, 1892.
- [7] I. S. Jacobs and C. P. Bean, "Fine particles, thin films and exchange anisotropy," in *Magnetism*, vol. III, G. T. Rado and H. Suhl, Eds. New York: Academic, pp. 271–350, 1963.
- [8] Y. Yorozu, M. Hirano, K. Oka, and Y. Tagawa, "Electron spectroscopy studies on magneto-optical media and plastic substrate interface," *IEEE Transl. J. Magn. Japan*, vol. 2, pp. 740–741, August 1987.
- [9] M. Young, *The Technical Writer's Handbook*. Mill Valley, CA: University Science, 1989.
- [10] J. Jiamei, and Z. Chunsheng, A novel Traveling Wave Ultrasonic Motor Using a Bar Shaped Transducer, J.Wuham University of Technology, 2008.
- [11] C.H. Yun, T. Ishii, K. Nakamura, S. Ueha, K. Akashi, A high power ultrasonic linear motor using a longitudinal and bending hybrid bolt-clamped Langevin type transducer, *Jpn. J. Appl. Phys.* 40 3773–3776, 2001.
- [12] F. Zhang, W.S. Chen, J.K. Liu, Z.S. Wang, Bidirectional linear ultrasonic motor using longitudinal vibrating transducers, *IEEE Trans. Ultrason. Ferroelectr. Freq. Control.* 52 (1) 134–138, 2005.
- [13] S.J. Shi, W.S. Chen, A bidirectional standing wave ultrasonic linear motor based on Langevin bending transducer, *Ferroelectrics* 350 102–110, 2008.
- [14] M. Shafik, J. A. G. Knight, H. Abdalla, (2001), "Development of a new generation of electrical discharge texturing system using an ultrasonic motor", 13th International Symposium for Electromachining, ISEM, Spain, May 9th to 11th, , 2001.
- [15] M. Shafik, J. A. G. Knight, H. Abdalla, "An investigation into electro discharge machining system applications using an ultrasonic motor", *Proceeding of ESM-2002 International Conference*, Belfast, August 28th to 31st, 2002.
- [16] M. Shafik & J. A. G. Knight, "Computer simulation and modelling of an ultrasonic motor using a single flexural vibrating bar", *Proceeding of ESM2002 International Conference*, Germany, June 3rd to 5th, 2002.
- [17] Shafik, M, 'Computer Aided Analysis and Design of a New Servo Control Feed Drive for EDM using Piezoelectric USM', PhD Thesis, De Montfort University, Leicester, UK, 2003.
- [18] M. Shafik, E. M. Shehaband H. S. Abdalla, 'A Linear Piezoelectric Ultrasonic Motor Using a Single Flexural Vibrating Transducer for Electro Discharge System Industrial Applications', *Int. J. Adv. Manuf. Technol.* 45:287–299, 2009.
- [19] He SY et al. "Standing wave bi-directional linearly moving ultrasonic motor", *IEEE trans. On Ultrasonics ferr. and freq. Control*, vol. 45, no. 5, 1998.
- [20] J. Satonobu, and J. R. Friend. Travelling Wave Excitation in a Flexural Vibration Ring by Using a Torsional-Flexural Composite Transducer, *IEEE Tran on Ultrasonics, Ferroelectrics and Frequency Control*, Vol. 48, No. 4, 2001
- [21] Tobias H., Jorg Wallaschek, "Survey of the present state of the art of piezoelectric linear motors", *Ultrasonics*, 38, 37-40, 2000.
- [22] Woo Seok Hwang and Hyun Chul Park. "Finite element modelling piezoelectric sensors and actuators", *AIAAJ*, Vol. 31, No. 5, 1993.
- [23] Y. Chikata, J. Oto, M. Onodera, M. Nishimura, 'Humidification Performance of Humidifying Devices for Tracheostomized Patients With Spontaneous Breathing: A Bench Study', *OPEN FORUM of the 58th AARC Congress*, held November 10–13, in New Orleans, Louisiana , 2012.
- [24] Y. Chikata, C. Sumida, J. Oto, H. Imanaka, and M. Nishimura, 'Humidification Performance of Heat and Moisture Exchangers for Pediatric Use', *Hindawi Publishing Corporation, Critical Care Research and Practice*, Volume 2012, Article ID 439267, 5 pages, 2012.
- [25] G. Eason, B. Noble, and I. N. Sneddon, "On certain integrals of Lipschitz-Hankel type involving products of Bessel functions," *Phil. Trans. Roy. Soc. London*, vol. A247, pp. 529–551, April 1955.
- [26] I. S. Jacobs and C. P. Bean, "Fine particles, thin films and exchange anisotropy," in *Magnetism*, vol. III, G. T. Rado and H. Suhl, Eds. New York: Academic, pp. 271–350, 1963.



#### BIOGRAPHICAL NOTES:

**A/Professor Mahmoud Shafik** is an international expert who has made a personal distinction and international leadership recognition, in the field of intelligent Mechatronics Systems and Technology with more than 20-years industrial applied research and development experience in Mechatronics Systems Hardware and Software, 3D Smart Actuators for Robotic Guidance and Machine Vision, Innovation for Sustainable Engineering, Advanced manufacturing technology, Sustainable design and innovation in products and manufacturing processes, Control and instrumentation, Sustainable rail transport infrastructure, Cancer Treatment using CVD Diamond Radio Therapy Technology, Information Technology for Blind and Visually Impaired people, Chronic Diseases Technological Solutions, TeleHealth, Telecare, Assisted Living Technology, Automation, Electric Cars-Steer by wire, AD-HOC wireless technology, CO2 and climate change, electro-rheological fluid micro actuators technology, software tools, and crises management and prevention.

Professor Shafik has been leading several European Commission and UK Research Council projects, of a budget of more than 20 million Euro's and have made a great economic and social impact in this area of expertise in UK and EU as a whole. His research work has brought many innovative outcomes that have been used commercially by a number of Small to Medium and Large enterprise organisations around the world, such as: Intersurgical Ltd – UK, Veslatec Oy – Finland, Semelab plc. – UK, PTW Freiburg – Germany, Neotek – France, Kirchlmaier Handel & Consulting GmbH – Austria, Spectrum Telecom Installations Ltd – Ireland, Diamond Materials GmbH – Germany, Fireworks International Ltd – UK, Pirotecnica Oscense SA – Spain, Total Motion Systems Ltd –UK, Micromech Limited – UK, Smart Technology Ltd – UK, Audi –Germany, Ford – UK, Schlumberger – France, Nissan – Japan and Rolls Royce - UK. For more information of Professor Shafik profile, career and achievements please visit: <https://www.linkedin.com/pub/mahmoud-shafik-ph-d/7/237/60>.